Time-Resolved Resonance Raman and Density Functional Theory Investigation of the Photoreactions of Benzophenone in Aqueous Solution

Yong Du, Jiadan Xue, Mingde Li, and David Lee Phillips*

Department of Chemistry, The University of Hong Kong, Pokfulam Road, Hong Kong, People's Republic of China

Received: December 18, 2008; Revised Manuscript Received: February 9, 2009

A time-resolved resonance Raman study of the photoreactions of benzophenone (BP) in neutral, alkaline, and acidic aqueous solutions is reported. Under neutral and alkaline conditions, a hydrogen abstraction reaction is observed to form the corresponding diphenyl ketyl (DPK) radical with different reaction rates while under acidic condition the protonation of triplet benzophenone occurs simultaneously, which is followed by a faster hydration reaction to produce the corresponding photohydration short-lived intermediates that were observed during experiments and that were tentatively assigned to the *m*-^{3}BP·H_2O and the *o*-^{1}BP·H_2O species. The dynamics, structures, and properties of these species are briefly discussed.

Introduction

The photophysical and photochemical properties of benzophenone (BP) have been intensely investigated since it is a prototypical aromatic ketone, and the photoreduction of BP has been of particular interest.[1−10] A deeper and more detailed understanding of the BP photophysics and photochemistry has been developed because of advances in technology and spectroscopic methods.[3−10] It has been established that the lowest excited triplet (T_1 nπ^*) is responsible for all of the major photophysical and photochemical reactions of BP in the solution phase.[11,12] The small energy gap and the strong spin−orbit coupling between BP's lowest excited singlet state (S_1 nπ^*) and its second excited triplet state (T_2 $\pi\pi^*$)[11,12] help the intersystem crossing (ISC) process to effectively compete kinetically with other S_1 state processes like internal conversion (IC) and fluorescence emission, so that the T_1 state is produced with a large yield close to unity, and hence the T_1 state is the precursor for subsequent processes and reactions. The T_1 state of BP can be efficiently photoreduced by hydrogen atom donors to produce a diphenyl ketyl (DPK) radical[13−15] that can then react with the other radical species like those formed from the H-donor solvent to produce long-lived light-absorbing transients (LAT). The LAT species in 2-propanol has been explicitly assigned to a 2-[4-(hydroxyl-phenyl-methylene)-cyclohexa-2,5-dienyl]-propan-2-ol cross-coupling product by using time-resolved resonance Raman (TR^3) spectroscopy measurements in conjunction with results from density functional theory calculations.[16]

While there have been many studies on the BP photoreduction reaction mechanism performed in a variety of organic solvents, fewer studies have examined the corresponding photochemical and photophysical processes in water which is considered to be a relatively "inert" hydrogen-donor solvent. Ledger and Porter[17] presented the first report that photolysis of BP in aqueous solution also generates the DPK radical through the hydrogen abstraction from water by a BP triplet (^{3}BP). In addition, they found that the phosphorescence of BP in aqueous solution is quenched by added protons although it remained unclear what caused this quenching.[17] In a recent study, Ramseier and co-workers[18] established that an acid-catalyzed photohydration is responsible for the triplet-quenching process observed in a moderately acidic aqueous solution (see Scheme 1). In this triplet-quenching process, the initial protonation of the carbonyl oxygen in ^{3}BP forms the corresponding excited triplet state conjugate acid (^{3}BP·H^+), and this species has its positive charge significantly delocalized at the ortho- and meta-positions of the benzene ring. On the basis of Zimmerman's "ortho-meta" effect for the benzene ring site activation in photochemical reactions,[19,20] these two sites bearing a positive charge can be attacked by water to produce short-lived hydration intermediates (*o*-^{3}BP·H_2O and *m*-^{3}BP·H_2O) that subsequently deactivate to the ground state (*o*-^{1}BP·H_2O) or proceed directly to the parent BP molecule by dehydration reactions.[18] A clear and definitive characterization of these transient species' kinetics and other properties by methods like transient absorption spectroscopy are hampered by overlapping of the broad featureless absorption bands of these species that exist on the same time scale. For example, the ^{3}BP·H^+ and the ^{3}BP·H_2O species are both anticipated to have a maximum absorption near ∼320 nm,[18] so there is some uncertainty on the assignment of these

SCHEME 1: Proposed Photohydation Reaction Pathways of Benzophenone in Aqueous Acid by Ramseier et al.[18]

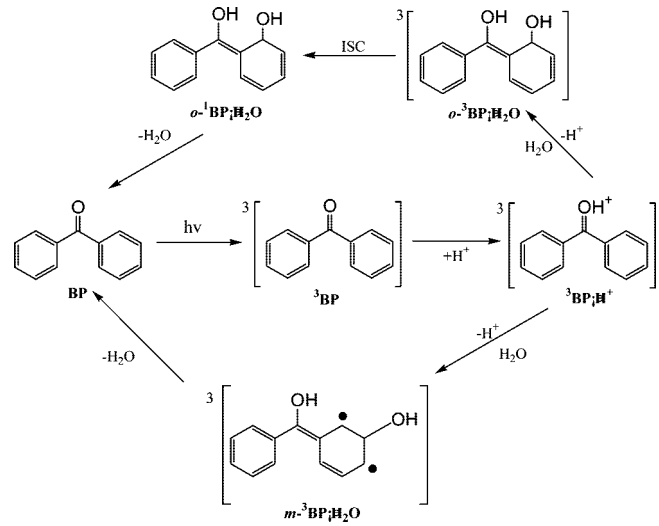

* To whom correspondence should be addressed. Telephone: 852-2859-2160. Fax: 852-2857-1586. E-mail: phillips@hkucc.hku.hk.

10.1021/jp811173x CCC: $40.75
Published on Web 03/12/2009

transient species using these methods. In addition, there appears to be no structural and vibrational information available in the literature concerning the photohydration reactions of BP and related aryl ketones. Time-resolved vibrational spectroscopic techniques like time-resolved resonance Raman (TR^3) spectroscopy can be used to unambiguously characterize and identify the transient species and to learn more about their structural and electronic properties. TR^3 spectroscopy can potentially be utilized to more clearly characterize the structural and dynamic properties of transient species even in cases where more than one transient species is present with similar overlapping absorption spectra as may be the case in the photohydration reactions of BP.

In this paper, TR^3 experiments were performed for BP in water:acetonitrile (1:1 by volume) mixed aqueous solutions under neutral, alkaline (containing 0.005, 0.05, and 0.25 M NaOH), and acidic (containing 0.5 and 3 M $HClO_4$) conditions to examine the transient species produced subsequent to the photoreactions of the triplet state in aqueous solutions under three typical solvent conditions. In neutral and alkaline solutions, hydrogen abstraction reactions were observed to form the corresponding DPK radical similar to the hydrogen abstraction reaction that occurs in 2-propanol solvent but with different reaction rates. However, in the acidic case, the protonation of the ^{3}BP takes place simultaneously with the hydrogen abstraction reaction and is followed by a faster hydration reaction to produce some short-lived intermediates in addition to the DPK radical formed from the hydrogen abstraction reaction. To our knowledge, this is the first TR^3 structural characterization of these intermediates and their dynamics for the photoreactions of BP in aqueous solution under neutral, alkaline, and acidic conditions. Density functional theory (DFT) calculations were performed using the (U)B3LYP method with a 6−311G** basis set to find the geometries and the vibrational frequencies for the species of interest here, and these results were compared to the TR^3 spectra to help make assignments to the experimental vibrational bands. The TR^3 spectra showed that the ^{3}BP hydrogen-abstraction reaction with water takes place to form DPK and OH radicals with a reaction rate slower than that for a 2-propanol solvent. In the acidic case, the ^{3}BP species was simultaneously protonated to generate a $^3BP{\cdot}H^+$ intermediate that can be easily attacked by water to form hydration products that were tentatively assigned to be the *m*-$^3BP{\cdot}H_2O$ and the *o*-$^1BP{\cdot}H_2O$ species.

Experimental and Computational Methods

Benzophenone (BP) was obtained from Aldrich (>99% purity), sodium hydroxide was obtained from UNI-Chem (>96% purity), and perchloric acid was acquired from ACS reagent ($HClO_4$ approx 70%). These compounds were used as received in conjunction with spectroscopic grade acetonitrile (MeCN) and deionized water solvents to prepare sample solutions for the experiments presented in this work.

Ns-TR^3 measurements were done using an experimental apparatus and methods that have been described previously,[21−26] so only a brief description will be given here. The fourth harmonic (266 nm) of a Spectra Physics LAB-170-10 Nd:YAG Q-switched laser supplied the pump wavelength, and the 319.9 nm probe wavelength came from the second Stokes hydrogen Raman shifted line pumped by the second harmonic (532 nm) from a second Nd:YAG laser (Spectra Physics GCR-150-10). A pulse delay generator was used to electronically control the time delay between the pump and probe laser beams which was monitored by a photodiode and a 500 MHz oscilloscope. The time resolution of our experiments was estimated to be ∼10 ns, and the energy of the pump and the probe pulses was in the 2.5−3.5 mJ range with a repetition rate of 10 Hz. A near collinear geometry was utilized to focus the pump and probe beams onto a flowing liquid stream of sample solution. The resonance Raman scattering was collected in a backscattering configuration and was detected by a liquid-nitrogen-cooled CCD detector that was mounted on an exit port of the monochromator. The ns-TR^3 measurements were performed under open air as well as under conditions where oxygen was bubbled through the sample solution. The Raman signal was acquired by the CCD detector for about 30∼60 s before being read out to an interfaced PC computer, and approximately 10−20 of these readouts were added together to obtain a resonance Raman spectrum. The spectra presented in this work were determined from subtraction of an appropriately scaled probe-before-pump spectrum from the corresponding pump−probe spectrum to remove solvent and precursor Raman bands. Acetonitrile Raman bands were used to calibrate the TR^3 spectra with an estimated accuracy of about ±3 cm^{-1} (and a relative accuracy of ±1−2 cm^{-1} from scan to scan) in absolute frequency. A Lorentzian function was used to integrate the relevant Raman bands in the TR^3 spectra so as to find their areas and to extract the decay and growth time constants of the species observed in the experiments.

The optimized geometries and vibrational frequencies for the ground and triplet states of the different probable species formed in the photoreactions studied were obtained from (U)B3LYP DFT calculations employing a 6−311G** basis set. No imaginary frequencies were observed at any of the optimized structures shown here. A Lorentzian function with a 20 cm^{-1} bandwidth was used in conjunction with the calculated Raman vibrational frequencies and their relative intensities to obtain the (U)B3LYP/6−311G** computed Raman spectra that were used to compare with corresponding relevant experimental TR^3 spectra. All of the calculations presented in this paper were done using the Gaussian 03[27] program suite installed on the High Performance Computing cluster at Computer Centre in The University of Hong Kong.

Results

A. TR^3 Spectroscopy of BP in Neutral and Alkaline Aqueous Solutions. Figure 1 displays nanosecond TR^3 spectra of BP in water:acetonitrile (1:1 by volume) mixed aqueous solution acquired with various time delays that are indicated next to the spectra. Inspection of Figure 1 shows that there are two major intermediates observed over the 0 ns to 2 μs time scale. The first species has characteristic Raman bands at 1542, 1470, 1213, and 971 cm^{-1} and appears to decay from 10 ns onward, and the decay of the first species appears to produce the second species. The second species which has characteristic Raman bands at 1582, 1553, 1484, 1272, 1187, 1117, 1023, and 990 cm^{-1} is generated within the resolution of the TR^3 experiments examined here (see the Raman band at 1582 cm^{-1} in the 0 ns TR^3 spectrum) and appears to first grow in and then disappears almost completely by 2 μs. The first species observed in the TR^3 spectra of Figure 1 is identified to be the triplet state of BP (^{3}BP) since it has a Raman spectrum that is essentially identical to that of the authentic ^{3}BP intermediate that was generated in acetonitrile solution and was detected with the same probe wavelength as used here (the comparison of these TR^3 spectra is shown in Figure 1S in the Supporting Information). Since acetonitrile is an inert solvent and only the photophysical processes occur from the triplet state after laser photolysis of

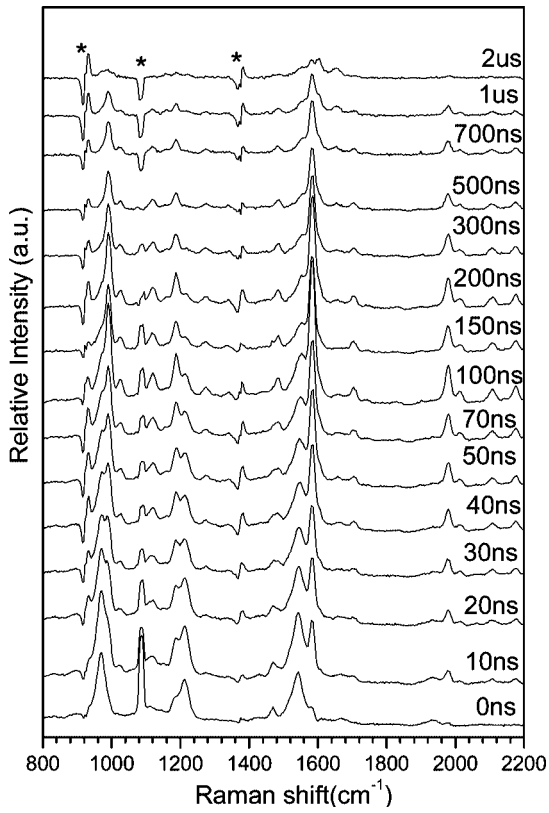

Figure 1. Nanosecond TR^3 spectra of BP in water:acetonitrile (1:1 by volume) obtained with 266 nm pump excitation wavelength and a 319.9 nm probe wavelength at various delay times that are indicated next to the spectra. The asterisk (*) symbols mark subtraction artifacts.

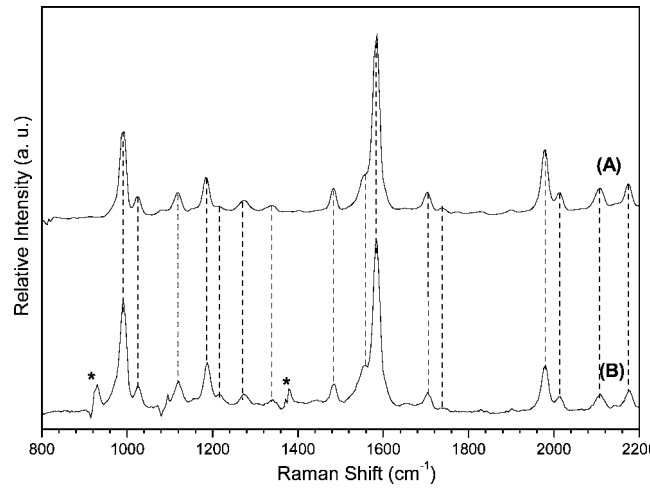

Figure 2. Comparison of Raman spectra of (A) the authentic DPK radical obtained in 2-propanol with (B) the second species obtained in neutral aqueous solution. Both spectra were acquired with a 319.9 nm probe wavelength after 266 nm photolysis of BP in the respective solvents. The asterisk (*) symbols mark subtraction artifacts.

BP because of its high ISC efficiency, the TR^3 spectra obtained in neat acetonitrile enable the clear characterization of ^{3}BP, which has been reported and discussed in detail previously.[16]

To remove the contributions from other intermediates including the ^{3}BP species and other species generated at post time delays, the Raman spectrum of the second species by itself was extracted by employing the spectrum of the ^{3}BP obtained in neat acetonitrile and by subtracting it from that acquired at 100 ns time delay in neutral aqueous solution as shown in Figure 1. This extracted Raman spectrum of the second species in neutral aqueous solution was compared to the Raman spectrum of the authentic DPK radical obtained in a 2-propanol solution,[16] and this comparison is shown in Figure 2. Examination of Figure 2 clearly shows that the spectrum of the second species is essentially identical to that of the DPK radical for all of more than 16 Raman bands that have noticeable intensity. This excellent agreement of the resonance Raman spectra clearly demonstrates that the two spectra in Figure 2 are due to the same species and that the second species observed on the nanosecond time scale in the neutral aqueous solution shown in Figure 1 is due to the DPK radical. Although the DPK radical is typically generated in H-donor solvents[13,14,16,28] such as alcohols and amines, the observation of the DPK radical here in neutral aqueous solution is in good agreement with previous results[17,29] that reported the observation of the DPK radical and is evidence for hydrogen abstraction from water by ^{3}BP.

The characteristic 1213 and 1582 cm^{-1} Raman features in Figure 1 for the ^{3}BP species and the DPK radical were fitted with Lorentzian band shapes to obtain the time dependences of these two species, and the kinetics obtained from this analysis is displayed in Figure 2S of the Supporting Information. The characteristic 1213 cm^{-1} Raman band for the ^{3}BP species was fitted with a single-exponential function with a time constant of 64 $\pm$ 3 ns. The characteristic 1582 cm^{-1} Raman band of the DPK radical was fitted with a two-exponential function with an $\sim$60 ns growth time constant and an $\sim$550 ns decay time constant. The time constants for the decay of ^{3}BP (64 $\pm$ 3 ns) and the growth of the DPK radical (60 ns) are close to each other within the uncertainty of the measurements, and this indicates that ^{3}BP is a precursor for the formation of the DPK radical. ^{3}BP has a lifetime of about 75 ns in neat acetonitrile[16] because of quenching by O_2. In neutral aqueous solution, the ^{3}BP decays by two parallel reaction pathways: one is quenched by O_2 and the other is trapped by hydrogen abstraction from a water molecule to form a DPK radical with a reaction rate k_2. The observed rate constant for the ^{3}BP decay in neutral aqueous solution is the sum of those determined by these two reaction pathways. We could not adequately sort out the different contributions to the overall observed decay of the ^{3}BP using the limited TR^3 data presented here, so a quantitative estimate of the rate constant for hydrogen abstraction from a water molecule to form a DPK radical is not given here.

The hydrogen abstraction from water by ^{3}BP produces an OH radical which then can attack BP to generate a cyclohexadienyl complex,[17] which is similar to the mechanism for producing the light-absorbing transients (LAT) species in 2-propanol.[16] In neutral aqueous solution examined here, as the DPK radical disappears, a new species is produced and is assigned to the 4-(hydroxyl-phenyl-methylene)-cyclohexa-2,5-dienol because it exhibits strong Raman features at 1654, 1604, and 1553 cm^{-1} that are very similar to those for 2-[4-(hydroxyl-phenyl-methylene)cyclohexa-2,5-dienyl]-propan-2-ol produced by a DPK radical reaction with the dimethylketyl radical.[16]

The TR^3 experiments for BP were also done in alkaline aqueous solution that contains 0.005, 0.05, and 0.25 M NaOH, and these TR^3 spectra are displayed in Figure 3 (the spectra obtained in 0.05 M NaOH solution) in the text and in Figure 3S (the spectra obtained in the 0.005 and 0.25 M NaOH solutions) in the Supporting Information. In these three alkaline aqueous solutions, both the ^{3}BP and the DPK radical were observed, and an interesting difference from the results obtained in a neutral aqueous solution is that the DPK radical decays somewhat faster in the alkaline solution (time constant = 370

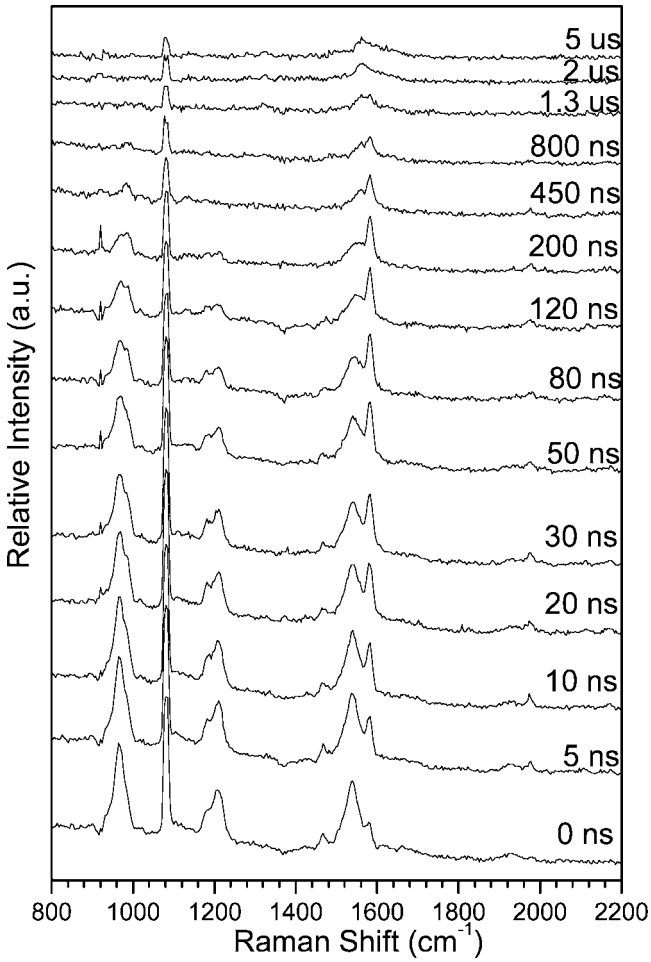

Figure 3. Nanosecond TR^3 spectra of BP in water:acetonitrile (1:1 by volume) that contains 0.05 M NaOH obtained with a 266 nm pump excitation wavelength and a 319.9 nm probe wavelength at various delay times indicated next to the spectra. The asterisk (*) symbols mark subtraction artifacts.

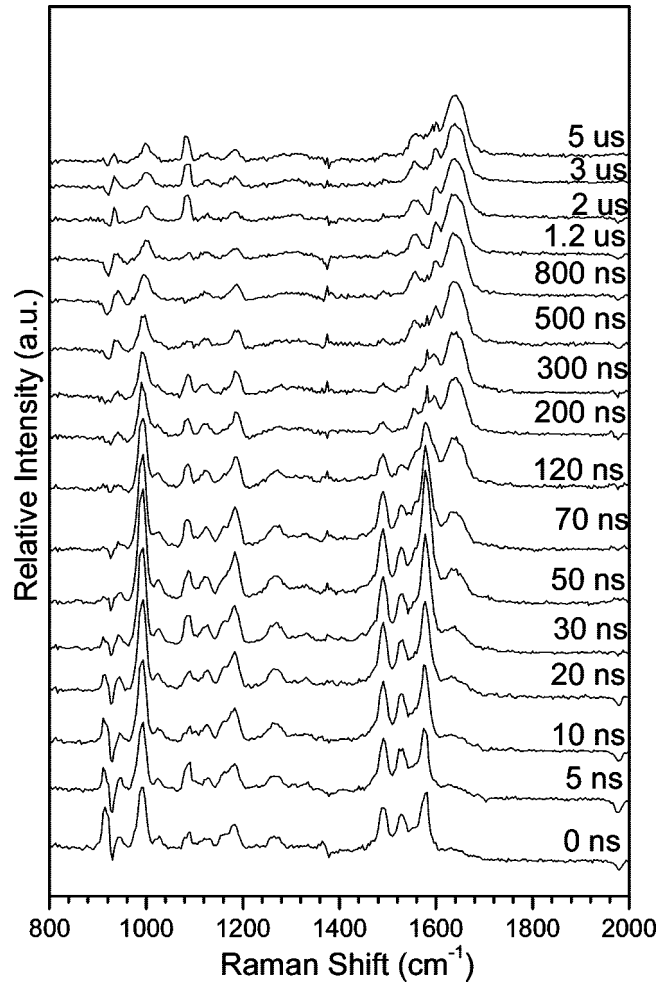

Figure 4. The extracted TR^3 spectra obtained from those acquired after photolysis of BP in the acidic aqueous solution (spectra shown in Figure 4S of the Supporting Information) by removing the contribution of the ^{3}BP and the DPK radical intermediates. All of the spectra were obtained with a 266 nm pump excitation wavelength and a 319.9nm probe wavelength. See the text for details.

ns) than in the neutral solution (time constant = 550 ns), and no strong Raman band appears to be produced at 1654 cm^{-1} that is characteristic of the LAT species formed from the reaction of the DPK radical with the OH radical in an aqueous solvent. This result suggests that the DPK radical has more reactivity toward the hydroxide ion than the OH radical and that the reaction of the DPK radical with the hydroxide ion tends to produce a radical anion species rather than a radical species.

B. Observation of the Photohydration Products after Photolysis of BP in Acidic Aqueous Solution. TR^3 spectra were obtained after 266 nm photolysis of BP in an acidic aqueous solution (water:acetonitrile (1:1 by volume) containing 0.5 M $HClO_4$) with a 319.9 nm probe wavelength at various time delays (these spectra are presented in Figure 4S of the Supporting Information). Since the protonation of the ground-state BP molecule is negligible in 5.8 M $HClO_4$ ($H_0 = -2.7$),[30] the molecule excited here should still be the ground state of BP. This is in agreement with our observation that the absorption of BP in the mixed aqueous solution containing 0.5 M $HClO_4$ matches that in the neutral aqueous solution. In Figure 4S of the Supporting Information, there are two new species produced on the 0 ns to 5 μs time scale in the acidic aqueous solution besides the ^{3}BP and the DPK radical intermediates that are predominant in the TR^3 spectra obtained after photolysis in a neutral aqueous solution. To clearly present the TR^3 spectra of the two new species and the kinetics relationship between them, the TR^3 spectra acquired in the acidic aqueous solution removed the contributions of the ^{3}BP and the DPK radical by subtracting an appropriately scaled Raman spectra of the ^{3}BP (the 10 ns spectrum obtained in the neat acetonitrile) and the DPK radical (the 70 ns spectrum obtained in 2-propanol), respectively. These extracted TR^3 spectra for the two new species are presented in Figure 4, and they have completely eliminated the influences of the ^{3}BP and the DPK radical species using the criterion of the Raman features at ~1000 cm^{-1} for the ^{3}BP and at ~1600 cm^{-1} for the DPK radical that are indicated with arrows in Figure 5S in the Supporting Information. Inspection of Figure 4 reveals that one new species with characteristic Raman bands at 1491, 1527, and 1574 cm^{-1} generates from 0 ns time delay and then decays to form the second new species that has its strongest Raman bands at 1560, 1596, and 1639 cm^{-1}, and this second new species remains stable up to 10 μs. There is some small probable contribution from the LAT species (e.g., the DPK radical and OH radical coupling complex) in the post time delays (e.g., those later than 800 ns) in Figure 4, but here it was omitted because of its small intensity since the amount of its precursor, the DPK radical in the acidic solution, is much smaller than that in the neutral solution.

The 1213 cm^{-1} Raman feature in Figure 4S of the Supporting Information for the ^{3}BP intermediate and for the 1491 and 1639

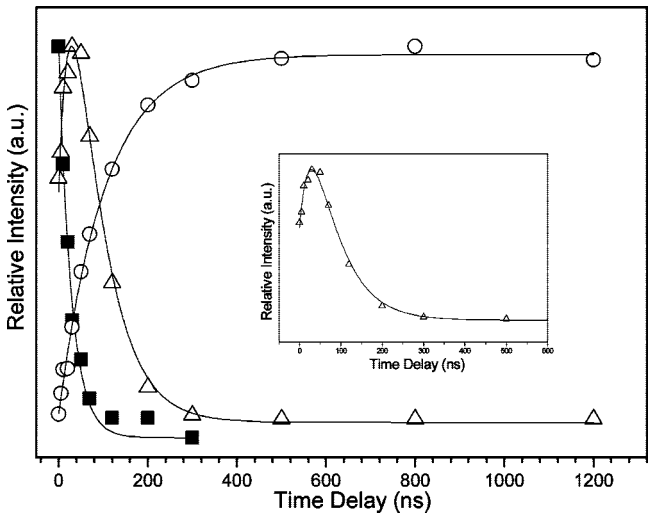

Figure 5. Time dependence of the 1213 cm^{-1} Raman band area of ^{3}BP (closed squares) fit with a single-exponential function with a decay time constant of 28 ± 2 ns. Time dependence of the 1491 cm^{-1} Raman band area of the first new species (open triangles) fit with a two-exponential function with an ~29 ns growth time constant and an ~63 ns decay time constant. Time dependence of the 1639 cm^{-1} Raman band area of the second new species (open circles) fit with a single-exponential function with a 105 ± 5 ns growth time constant. The inset displays an expanded view of the 1491 cm^{-1} kinetics during the first 600 ns. The data displayed here were derived from the TR^3 spectra shown in Figure 4 and in Figure 4S of the Supporting Information (see the text for more details).

cm^{-1} Raman features for the first and second new species in Figure 4 were fitted with Lorentzian band shapes to obtain the time dependences of these three species, and the kinetics obtained is displayed in Figure 5. The 1213 cm^{-1} Raman band for the ^{3}BP was fitted with a single-exponential function with a time constant of 28 ± 2 ns, and the 1491 cm^{-1} Raman band area of the first new species was fitted with a two-exponential function with ~29 ns growth time constant and ~63 ns decay time constant. The growth of the 1639 cm^{-1} Raman band area for the second new species was fitted better with a single-exponential function than with a two-exponential function, and the single-exponential function has a 105 ± 5 ns growth time constant. The time constants for the decay of ^{3}BP (28 ± 2 ns) and for the growth of the first new species (~29 ns) are close to each other within the uncertainty of the measurements, and this indicates that the ^{3}BP intermediate is a precursor for the formation of the first new species (1491 cm^{-1}) that is unstable and that further decays. However, the decay of the first new species is much faster than the growth of the second new species (1639 cm^{-1}), and hence they do not appear to be correlated with each other within the experimental error. This will be discussed in detail in a subsequent section.

The ^{3}BP intermediate is easy to be protonated in the moderately acidic solution to form the $3BP \cdot H^+$ species which is unstable and which can be attacked by water to produce a triplet hydration product. Ramseier et al. reported[18] that the $^3BP \cdot H_2O$ species observed with a maximum absorption at 315 nm was assigned to have the meta structure mainly relying on the high-yield generation of meta-hydroxy derivatives after photolysis of the fluoride-substituted acetophenone and benzophenone compounds. Here, the first new species that was generated in the acidic aqueous solution as shown in Figure 4 is also tentatively assigned to the *m*-$^3BP \cdot H_2O$. Figure 6 shows the DFT calculation (UB3LYP/6−311G**) predicted Raman spectra for the *m*-$^3BP \cdot H_2O$ species whose structures with

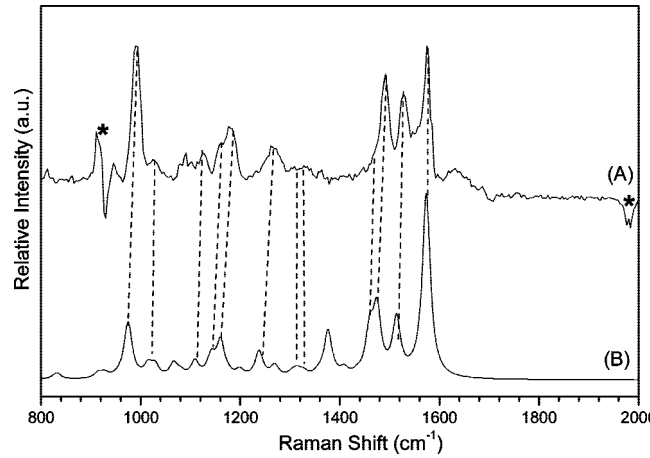

Figure 6. Comparison of (A) the extracted Raman spectrum for the first new species obtained in the acidic aqueous solution with (B) the DFT calculation predicted Raman spectrum for the excited triplet hydration product, *m*-^{3}BP H_2O. The asterisk (*) symbols mark subtraction artifacts.

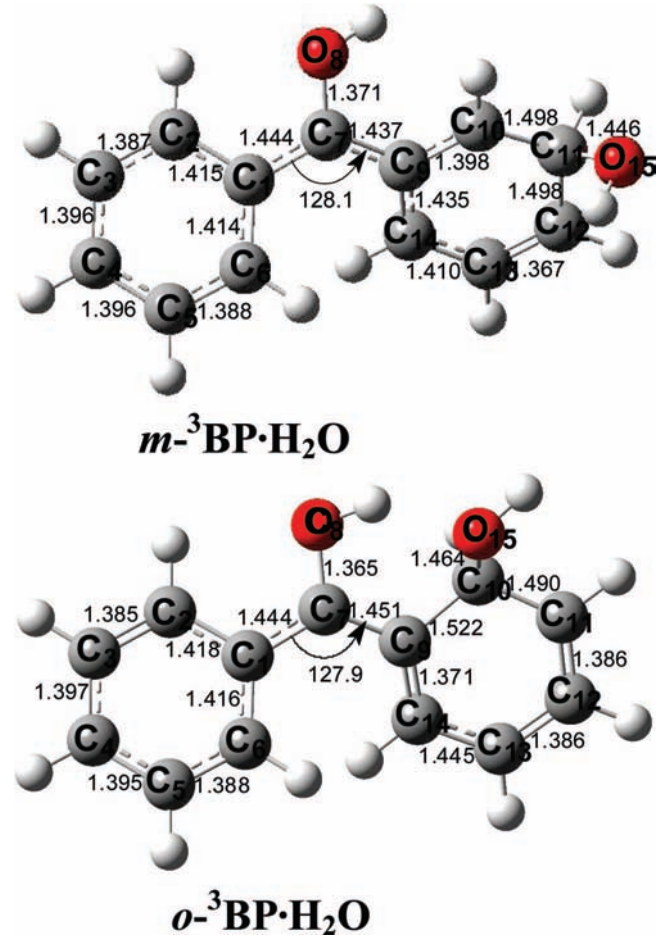

Figure 7. Optimized structures of the *m*-$^3BP \cdot H_2O$ and the *o*-$^3BP \cdot H_2O$ species calculated from the UB3LYP/6−31G** DFT calculations. Selected bond lengths (in Å) and bond angles (in deg) are labeled.

selected bond lengths are presented in Figure 7. Table 1S in the Supporting Information presents the tentative vibrational assignments and a nominal description of the normal modes for the hydration product. Most of the fundamental Raman bands observed for the TR^3 spectra of the *m*-$^3BP \cdot H_2O$ species are due to vibrations associated with the aromatic ring C−C stretch, the C−H bend motions, and the benzene ring deformation. For example, the 1407, 1491, 1531, 1549, and 1575 cm^{-1} vibrational

bands have major contributions from the aromatic ring C−C stretch motions while the 1128, 1161, 1269, and 1237 cm^{-1} vibrational bands have major contributions from the C−H in-plane bend motions, and the 990 and 1027 cm^{-1} bands have major contributions from the benzene ring deformation motions. Examination of Figure 6 and Table 1S in the Supporting Information reveals that the calculated vibrational frequencies for the *m*-^{3}BP•H_2O product agree well with the experimentally observed TR^3 Raman bands for the first new species. For example, the calculated frequencies for the *m*-^{3}BP•H_2O product are within about 7 cm^{-1} on average for the 12 experimental TR^3 Raman band frequencies for the first new species. The experimental and calculated spectrums in Figure 6 show moderate differences in their relative Raman intensity pattern, and this can be readily accounted for by the experimental spectrum being resonantly enhanced while the calculated spectrum is nonresonant Raman spectrum.

The predicted excited-state energies and oscillator strengths from TD-DFT (UB3LYP/6−311G**) calculations for the *m*-^{3}BP•H_2O and the *o*-^{3}BP•H_2O shown in Table 2S (see Supporting Information) are consistent with the assignment of the first new species in the acidic aqueous solution to the *m*-^{3}BP•H_2O. For example, the calculations in Table 2S predict the strongest transition for *m*-^{3}BP•H_2O to be at 311 nm with an oscillator strength of 0.24. This result is consistent with our TR^3 spectra obtained in the acidic aqueous solution for the first new species using a 319.9 nm probe wavelength that is localized in the region of the maximum absorption of the *m*-^{3}BP•H_2O species. However, the TD-DFT (UB3LYP/6−311G**) calculations predicted that the *o*-^{3}BP•H_2O has its strongest transition at 387 nm with an oscillator strength of 0.24 while those close to the probe wavelength used here are at 333 and 314 nm and have oscillator strengths of only 0.013 and 0.0043, respectively. This result can probably account for the fact that although the *o*-^{3}BP•H_2O is also likely produced during the reaction, its Raman signal was not detected in our present TR^3 experiments since it does not have a strong electronic transition at our 319.9 nm probe excitation wavelength.

The *m*-^{3}BP•H_2O species has a shorter lifetime than that of the *o*-^{3}BP•H_2O species, and *m*-^{3}BP•H_2O will return to the ground state of BP by elimination of a water molecule, while the *o*-^{3}BP•H_2O species would be anticipated to form the ground state of BP through the ground-state hydration product *o*-^{1}BP•H_2O that has a long-lived lifetime of several minutes and can be isolated as shown in Scheme 1.[10,18] Here, the observation of two new species produced in the acidic aqueous solution and the result that the growth of the second new species is much slower than the decay of the first new one that has been tentatively identified as *m*-^{3}BP•H_2O strongly support the assignment of the second species to be the *o*-^{1}BP•H_2O. To verify the *o*-^{1}BP•H_2O assignment for the second species observed in the TR^3 spectra of Figure 4, DFT calculations were performed, and these results were compared to the experimental TR^3 spectrum obtained at 2 μs in Figure 7S of the Supporting Information that was obtained by subtracting the signals of the ^{3}BP and the DPK radical intermediates from those acquired in a 3 M $HClO_4$ aqueous solution. Figure 8 displays a comparison of the experimental TR^3 spectrum to the B3LYP/6−311G** calculated normal Raman spectrum of the *o*-^{1}BP•H_2O species. Preliminary Raman band assignments for the *o*-^{1}BP•H_2O species were made on the basis of the correlation between the experimental and the calculated Raman spectra shown in Figure 8, and Table 3S in the Supporting Information lists these tentative vibrational assignments with nominal descriptions of the normal modes. Six major Raman bands, at 997, 1191, 1603, 1632, 1653, and 1682 cm^{-1}, were observed; most of the Raman bands seen in the TR^3 spectra of the *o*-^{1}BP•H_2O species are due to vibrations associated with the ring C−C stretch and O−H bend motions. Examination of Figure 8 and Table 3S indicates that the calculated Raman spectrum for the *o*-^{1}BP•H_2O species agrees well with the experimental vibrational frequencies for the second species observed at post time delays in the acidic aqueous solution with only about 6 cm^{-1} on average frequency difference for the six vibrational modes observed.

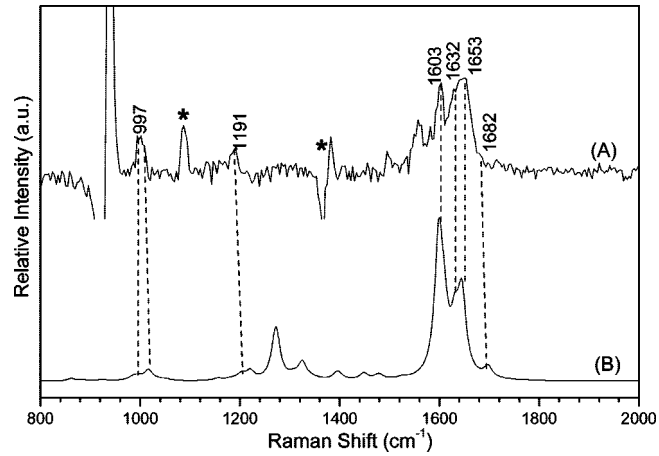

Figure 8. Comparison of (A) the experimental TR^3 spectrum that was obtained by subtracting the signals of the ^{3}BP and the DPK radical species from the TR^3 spectra acquired in 3 M $HClO_4$ aqueous solution to (B) the (U)B3LYP/6−311G** calculated normal Raman spectrum of the *o*-^{1}BP•H_2O species. The asterisk (*) symbols mark subtraction artifacts.

The TR^3 experiments were also performed for BP in a more acidic aqueous solution that contains 3 M $HClO_4$, and these TR^3 spectra are displayed in Figure 6S of the Supporting Information. The same species (including ^{3}BP, *m*-^{3}BP•H_2O, and *o*-^{1}BP•H_2O) were observed in the 3 M $HClO_4$ aqueous solution, but the dynamics of these species was found to be different from those obtained in the 0.5 M $HClO_4$ aqueous solution. For example, the ^{3}BP has been completely quenched within 5 ns, and the *m*-^{3}BP•H_2O species has accumulated to its maximum at 0 ns and begins to decay from 0 ns. This result is in agreement with the expectation that the protonation of the triplet state of BP, ^{3}BP•H^+, attacked by water is responsible for the decay of the triplet BP (^{3}BP).[18] The Raman band intensity for the *o*-^{1}BP•H_2O species (see the 2 μs spectrum in Figure 7S of the Supporting Information) is not as big as that in Figure 4 that was acquired in the 0.5 M $HClO_4$ aqueous solution, and this may be mainly due to the triplet−triplet annihilation that would be anticipated to easily occur when the concentration of the triplet species is as high as that examined here.[31]

Discussion

A. DPK Radical in the Neutral and Alkaline Aqueous Solutions. The DPK (diphenyl ketyl) radical is well-known to be generated from the reaction of the ^{3}BP intermediate with alcohols like 2-propanol and has been clearly characterized by a transient absorption spectrum[32] that shows that the DPK radical has absorption bands at 330 and 540 nm and TR^3 spectra[16] containing specific vibrational and structural information. Flash photolysis of BP in water also observed an absorption at 330 and 540 nm, and this species was assigned to the DPK radical.[17] Here, the satisfactory agreement of the transient resonance Raman spectrum for the new species that is generated with the

decay of the triplet BP in a neutral aqueous solution with the authentic Raman spectrum of the DPK radical that was obtained in 2-propanol under the same experimental conditions definitely demonstrates that the new species is the DPK radical. The generation of the DPK radical in the neutral aqueous solution is not due to the reaction of ^{3}BP with the ground-state BP or with ^{3}BP itself since the formation rate of the DPK radical in our experiments is not dependent on the concentration of the BP precursor or the pump power used during the TR^3 experiments. Our TR^3 results indicate that the ^{3}BP decays by a first-order kinetics to form the DPK radical, since the time constants for the decay of ^{3}BP (64 ± 3 ns) and the growth of DPK radical (~60 ns) are close to each other within the uncertainty of the measurements, and this result is also in agreement with previous work[17,29] that observed that an absorption was left at 330 and 540 nm after the decay of some absorption at 315 and 525 nm. The ^{3}BP intermediate has its maximum absorption at 315 and 525 nm and overlaps with the absorption of the DPK radical, and it is therefore difficult from the transient absorption spectra to directly obtain reliable dynamic information for these two correlated species.

The generation of the DPK radical is due to the hydrogen abstraction by the ^{3}BP from water that simultaneously produces OH radicals, and these OH radicals may then attack the DPK radical to form a cyclohexadienyl complex.[17] Here, the cyclohexadienyl complex appears to have a similar structure to that of the LAT species[16] observed in the neutral aqueous solution. Figure 8S in the Supporting Information presents a comparison of the Raman spectra of the species (the 2 μs TR^3 spectrum in Figure 1 subtracting the scaled Raman spectrum for the DPK radical) that was observed after the decay of the DPK radical to the LAT species acquired in the 2-propanol and detected using the same probe wavelength and the DFT calculation predicted Raman spectrum for the *para*-DPK-OH complex. The four strong Raman features for the cross-coupling species agree very well with those of the LAT species, and they are observed at around 1654, 1604, 1571, and 1553 cm^{-1}. This is not surprising since these four Raman features correspond to the aromatic ring C−C stretching, and the attachment of the OH radical or the dimethylketyl radical at the para site of the benzene ring does not change the cyclohexadienyl character of the benzene ring so much. The DFT calculations for the geometry of the *para*-DPK-OH complex (see Figure 9S in the Supporting Information) also support this assignment. The observation of the *para*-DPK-OH complex provides further support that water is able to donate a hydrogen atom to the ^{3}BP intermediate to form a DPK radical.

In the alkaline aqueous solution, the DPK radical was produced while the ^{3}BP decays, and the DPK radical was identified by comparison with the Raman spectrum of an authentic spectrum of the DPK radical obtained in 2-propanol as shown in Figure 10S of the Supporting Information (the Raman spectrum was obtained using the 50 ns TR^3 spectrum in the alkaline aqueous solution of Figure 3 and subtracting an appropriately scaled Raman spectrum of the ^{3}BP species, and the resulting spectrum agrees well with that for the authentic DPK radical). The observation of the DPK radical in the alkaline aqueous solution is not inconsistent with the Ledger and Porter result[17] that flash photolysis of BP in a 0.05 N NaOH solution produced the ^{3}BP that then decayed to leave a species absorbing at 335 and 600 nm that was assigned to the radical ion of BP. The DPK radical has an absorption feature at 330 nm, and this could possibly overlap with the absorptions at 315 and 335 nm that correspond to the ^{3}BP species and a new radical ion species.

B. Rate Constants for BP Hydration Products in Acidic Aqueous Solution. All of the TR^3 experiments performed here are under open air conditions, and the solubility of O_2 in acetonitrile is larger than that in water, so the influence of O_2 on the triplet BP cannot be omitted. The 75 ns lifetime[16] for the ^{3}BP in neat acetonitrile is predominantly due to the O_2 quenching. The ^{3}BP in the acidic aqueous solution was observed to decay through three main parallel pathways including O_2 quenching, hydrogen abstraction from water to form the DPK radical, and protonation to give the ^{3}BP•H$^+$ species that is quickly attacked by water to generate the ^{3}BP•H$_2$O species. Assuming that the concentrations of O_2, water, and protons in the solution are constant during the photoreaction, then some reactions can be treated with first-order kinetics. The formation rate constant for the ^{3}BP•H$_2$O was estimated here to be 2×10^7 s^{-1} under the condition of [H$^+$] at 0.5 M. This result is consistent with the time constants for the formation of ^{3}BP•H$^+$ reported by Ramseier et al. of $(2.2 \pm 0.3) \times 10^7$ s^{-1} with 0.1 M protons and $(5 \pm 1) \times 10^8$ s^{-1} with 1.0 M protons.[18] In the 3 M HClO$_4$ aqueous solution examined in our TR^3 experiments, the ^{3}BP•H$_2$O was observed to accumulate to its maximum amount at 0 ns time delays, and this magnitude agrees well with the result that the ^{3}BP•H$^+$ forms with the rate of $(10.9 \pm 0.7) \times 10^8$ s^{-1} with the H$^+$ concentration of 3.0 M.[18] The TR^3 results obtained in the 0.5 M HClO$_4$ aqueous solution show that the decay of the ^{3}BP intermediate is correlated with the growth of the ^{3}BP•H$_2$O species, and no new resonance Raman signals can be detected between these two species. This is mainly due to the hydration of the ^{3}BP•H$^+$ species in moderately concentrated aqueous acids, with a rate constant of 1.5×10^9 s^{-1},[18] that is much faster than the formation of the ^{3}BP•H$^+$ species. The ^{3}BP•H$_2$O species (which is assigned to *m*-^{3}BP•H$_2$O) was observed to disappear with a time constant of about 63 ns in the 0.5 M acid solution, so the rate constant of 1.5×10^7 s^{-1} agrees well with the corresponding value of $(2.0 \pm 0.1) \times 10^7$ s^{-1} obtained by Ramseier et al.[18]

C. Structures of the Triplet BP Hydration Products. The structures and properties of the *m*-^{3}BP•H$_2$O and the *o*-^{3}BP•H$_2$O are significantly different from one another, and Figure 7 presents some selected bond lengths and bond angles for these two hydration triplet products. Inspection of the structures shown in Figure 7 reveals that the attack by water at different sites of the benzene ring makes the structures of the corresponding benzene ring in the two triplet hydration products significantly different from each other. For example, the lengths of the C9−C10, C11−C12, and C9−C14 bonds are 1.398, 1.498, and 1.435 Å for the *m*-^{3}BP•H$_2$O species, while for the *o*-^{3}BP•H$_2$O species, the corresponding bonds lengths are 1.522, 1.386, and 1.371 Å, respectively. This distinction makes the *m*-^{3}BP•H$_2$O species have more cyclohexadienyl-like character while the *o*-^{3}BP•H$_2$O does not have as much. This means that the *m*-^{3}BP•H$_2$O species has substantial alternation of the C−C bond lengths of the aromatic ring. The molecules with cyclohexadienyl character are reflected in the resonance Raman spectra to have strong vibrational bands at around 1600 cm^{-1} corresponding to the aromatic ring C−C stretching. For example, the LAT species[16] and the arylnitrenium ions[22,24,33,34] previously studied with time-resolved vibrational spectroscopy have strong Raman features observed at around 1600 cm^{-1} that correspond to the aromatic ring C−C stretching motions, and the DFT calculations for their geometries revealed that they all have significant cyclohexadienyl character. Here, the observed resonance Raman spectrum for the *m*-^{3}BP•H$_2$O species is consistent with its cyclohexadienyl character.

Conclusion

A nanosecond time-resolved resonance Raman (ns-TR^3) spectroscopic investigation of the reactions of the triplet benzophenone (^3BP) species in the neutral, alkaline, and acidic aqueous solutions was described. The TR^3 spectra showed that the ^3BP hydrogen abstraction reaction with water occurred to produce a DPK radical and OH radicals with a reaction rate slower than that with a 2-propanol solvent. However, in the acidic case, the ^3BP species was simultaneously protonated to generate the $^3BP{\cdot}H^+$ intermediate that is unstable and that can be easily attacked by water to produce the hydration products that were tentatively assigned to be the *m*-$^3BP{\cdot}H_2O$ and the *o*-$^1BP{\cdot}H_2O$ species on the basis of previous results in the literature and results from DFT calculations. The TR^3 spectra obtained under acidic aqueous condition fully confirm and further establish previous conclusions drawn from transient absorption spectroscopy.[18]

Acknowledgment. This work was supported by a grant from the Research Grants Council of Hong Kong (HKU 7035/08P), the award of a Croucher Foundation Senior Research Fellowship (2006-07) from the Croucher Foundation, and an Outstanding Researcher Award (2006) from the University of Hong Kong to D. L. P.

Supporting Information Available: Figure 1S: 0 ns TR^3 spectrum in neutral aqueous solution (A) compared with a TR^3 spectrum of authentic triplet BP (B) that was obtained in pure acetonitrile solvent. Figure 2S: Time dependence of the 1213 cm^{-1} Raman band of the ^3BP (open triangles) fit with a single-exponential function with a time constant of 64 ± 3 ns. Time dependence of the 1582 cm^{-1} Raman band area of DPK (open circles) fit with a two-exponential function with ~60 ns growth time constant and ~550 ns decay time constant. The data displayed here were derived from the TR^3 spectra shown in Figure 1. Figure 3S: Nanosecond TR^3 spectra of BP in BP in water:acetonitrile (1:1 by volume) that contains 0.005 and 0.25 M NaOH obtained with a 266 nm pump excitation wavelength and a 319.9 nm probe wavelength at various delay times indicated next to the spectra. Figure 4S: TR^3 spectra of BP in acidic aqueous solution (containing 0.5 M $HClO_4$) obtained with a 266 nm pump excitation wavelength and a 319.9 nm probe wavelength at various delay times indicated next to the spectra. Figure 5S: (black) Raman spectrum of the transient species obtained at 10 ns after 266 nm photolysis of BP in the aqueous solution containing 0.5 M $HClO_4$ and a (red) scaled spectrum of the ^3BP obtained in neat acetonitrile and a (blue) scaled spectrum of the DPK radical obtained in 2-propanol. All of these three spectra were obtained under the same experimental conditions. Figure 6S: TR^3 spectra of BP in acidic aqueous solution (containing 3 M $HClO_4$) obtained with a 266 nm pump excitation wavelength and a 319.9 nm probe wavelength at various delay times indicated next to the spectra. Figure 7S: Extracted TR^3 spectra obtained by removing the contributions of the ^3BP and the DPK radical spectra from spectra obtained after photolysis of BP in the acidic aqueous solution containing 3 M $HClO_4$ (Figure 6S). All spectra were obtained with a 266 nm pump excitation wavelength and a 319.9 nm probe wavelength. Figure 8S: Comparison of the (A) DFT calculation predicted Raman spectrum for the *para*-DPK-OH complex and the (B) TR^3 spectrum for the species observed after the decay of the DPK radical in the neutral aqueous solution and the (C) LAT species obtained after photolysis in the 2-propanol. Figure 9S: Optimized structures of the *para*-DPK-OH complex calculated from the B3LYP/6−31G** DFT calculations. Selected bond lengths (in Å) and bond angles (in deg) are labeled. Figure 10S: Comparison of (A) the authentic DPK radical TR^3 spectrum obtained in 2-propanol with (B) the second species TR^3 spectrum obtained from the 50 ns TR^3 spectrum (Figure 3S) in the alkaline aqueous solution and subtracting the scaled TR^3 spectrum for the ^3BP species. Table 1S: Raman frequencies (in cm^{-1}) and assignments for the *m*-$^3BP{\cdot}H_2O$ species. Table 2S: Excited-state energies and oscillator strengths from the TD-DFT (UB3LYP/6−311G**) calculations for the two photohydration triplet species, *o*-$^3BP{\cdot}H_2O$ and *m*-$^3BP{\cdot}H_2O$. Table 3S: Raman frequencies (in cm^{-1}) and assignments for the *o*-$^1BP{\cdot}H_2O$ species. Cartesian coordinates, total energies, and vibrational zero-point energies for the optimized geometries obtained from the (U)B3LYP/6−31G** calculations for the *o*-$^3BP{\cdot}H_2O$, *m*-$^3BP{\cdot}H_2O$, and the *o*-$^1BP{\cdot}H_2O$ species. This material is available free of charge via the Internet at http://pubs.acs.org.

References and Notes

(1) Hammond, G. S.; Moore, W. M. *J. Am. Chem. Soc.* **1959**, *81*, 6334–6334.
(2) Moore, W. M.; Hammond, G. S.; Foss, R. P. *J. Am. Chem. Soc.* **1961**, *83*, 2789–2794.
(3) Rentzepis, P. M. *Science* **1970**, *169*, 239–247.
(4) Anderson, J., R. W.; Hochstrasser, R. M.; Lutz, H.; Scott, G. W. *J. Chem. Phys.* **1974**, *61*, 2500–2506.
(5) Peters, K. S.; Freilich, S. C.; Schaeffer, C. G. *J. Am. Chem. Soc.* **1980**, *102*, 5701–5702.
(6) Wagner, P. J.; Truman, R. J.; Scaiano, J. C. *J. Am. Chem. Soc.* **1985**, *107*, 7093–7097.
(7) Bhasikuttan, A. C.; Singh, A. K.; Palit, D. K.; Sapre, A. V.; Mittal, J. P. *J. Phys. Chem. A* **1998**, *102*, 3470–3480.
(8) Huck, L. A.; Wan, P. *Org. Lett.* **2004**, *6*, 1797–1799.
(9) Mitchell, D.; Lukeman, M.; Lehnherr, D.; Wan, P. *Org. Lett.* **2005**, *7*, 3387–3389.
(10) Basaric, N.; Mitchell, D.; Wan, P. *Can. J. Chem.* **2007**, *85*, 561–571.
(11) Shah, B. K.; Rodgers, M. A. J.; Neckers, D. C. *J. Phys. Chem. A* **2004**, *108*, 6087–6089.
(12) Shah, B. K.; Neckers, D. C. *J. Am. Chem. Soc.* **2004**, *126*, 1830–1835.
(13) Tahara, T.; Hamaguchi, H.; Tasumi, M. *Chem. Phys. Lett.* **1988**, *152*, 135–139.
(14) Tahara, T.; Hamaguchi, H.; Tasumi, M. *J. Phys. Chem.* **1990**, *94*, 170–178.
(15) Yabumoto, S.; Sato, S.; Hamaguchi, H. *Chem. Phys. Lett.* **2005**, *416*, 100–103.
(16) Du, Y.; Ma, C.; Kwok, W. M.; Xue, J.; Phillips, D. L. *J. Org. Chem.* **2007**, *72*, 7148–7156.
(17) Ledger, M. B.; Porter, G. *J. Chem. Soc., Faraday Trans. 1* **1972**, *68*, 539–553.
(18) Ramseier, M.; Senn, P.; Wirz, J. *J. Phys. Chem. A* **2003**, *107*, 3305–3315.
(19) Zimmerman, H. E. *J. Am. Chem. Soc.* **1995**, *117*, 8988–8991.
(20) Zimmerman, H. E. *J. Phys. Chem. A* **1998**, *102*, 5616–5621.
(21) Du, Y.; Guan, X.; Kwok, W. M.; Chu, L. M.; Phillips, D. L. *J. Phys. Chem. A* **2005**, *109*, 5872–5882.
(22) Zhu, P.; Ong, S. Y.; Chan, P. Y.; Leung, K. H.; Phillips, D. L. *J. Am. Chem. Soc.* **2001**, *123*, 2645–2649.
(23) Chan, P. Y.; Ong, S. Y.; Zhu, P.; Zhao, C.; Phillips, D. L. *J. Phys. Chem. A* **2003**, *107*, 8067–8074.
(24) Xue, J.; Chan, P. Y.; Du, Y.; Guo, Z.; Chung, C. W. Y.; Toy, P. H.; Phillips, D. L. *J. Phys. Chem. B* **2007**, *111*, 12676–12684.
(25) Du, Y.; Xue, J.; Ma, C.; Kwok, W. M.; Phillips, D. L. *J. Raman Spectrosc.* **2008**, *39*, 503–514.
(26) Xue, J.; Du, Y.; Guan, X.; Guo, Z.; Phillips, D. L. *J. Phys. Chem. A* **2008**, *112*, 11582–11589.
(27) Frisch, M. J.; Trucks, G. W.; Schlegel, H. B.; Scuseria, G. E.; Robb, M. A.; Cheeseman, J. R.; Zakrzewski, V. G.; Montgomery, J. A., Jr.; Stratmann, R. E.; Burant, J. C.; Dapprich, S.; Millam, J. M.; Daniels, A. D.; Kudin, K. N.; Strain, M. C.; Farkas, O.; Tomasi, J.; Barone, V.; Cossi, M.; Cammi, R.; Mennucci, B.; Pomelli, C.; Adamo, C.; Clifford, S.; Ochterski, J.; Petersson, G. A.; Ayala, P. Y.; Cui, Q.; Morokuma, K.; Malick, D. K.; Rabuck, A. D.; Raghavachari, K.; Foresman, J. B.; Cioslowski, J.; Ortiz, J. V.; Baboul, A. G.; Stefanov, B. B.; Liu, G.; Liashenko, A.; Piskorz, P.; Komaromi, I.; Gomperts, R.; Martin, R. L.; Fox, D. J.; Keith, T.; Al-Laham, M. A.; Peng, C. Y.; Nanayakkara, A.; Gonzalez, C.; Challacombe, M.; Gill,

P. M. W.; Johnson, B.; Chen, W.; Wong, M. W.; Andres, J. L.; Gonzalez, C.; Head-Gordon, M.; Replogle, E. S.; Pople, J. A. *Gaussian 98*, revision A.7, and *Gaussian 03*, revision B.05; Gaussian Inc.: Pittsburgh, PA, 1998, 2003.

(28) Tahara, T.; Hamaguchi, H.; Tasumi, M. *J. Phys. Chem.* **1987**, *91*, 5875–5880.

(29) Bensasson, R. V.; Gramain, J.-C. *J. Chem. Soc., Faraday Trans. 1* **1980**, *76*, 1801–1810.

(30) Kresge, A. J.; Chen, H. J.; Capen, G. L.; Powell, M. F. *Can. J. Chem.* **1983**, *61*, 249–256.

(31) Turro, N. J. *Modern Molecular Photochemistry*; University Science Books: Mill Valley, CA, 1991.

(32) Fox, R.; Sherwood, J. N. *Trans. Faraday Soc.* **1971**, *67*, 3364–3371.

(33) Chan, P. Y.; Ong, S. Y.; Zhu, P.; Zhao, C.; Phillips, D. L. *J. Phys. Chem. A* **2003**, *107*, 8067–8074.

(34) Chan, P. Y.; Kwok, W. M.; Lam, S. K.; Chiu, P.; Phillips, D. L. *J. Am. Chem. Soc.* **2005**, *127*, 8246–8247.

JP811173X